

An investigation of shell-helical coiled tube heat exchanger used for solar water heating system

.Karima E. Amori * Jinan Shaker Sherza

Univ. of Baghdad/ Mech. Eng. Dept. , Baghdad-Iraq

* E-mail of the corresponding author: drkarimaa63@gmail.com, drkarimaa@yahoo.com

Abstract

An experimental and theoretical study has been performed of thermal and hydrodynamic characteristics of a new type shell-helical coiled tube heat exchanger used as a storage tank in a closed loop solar water heater system for no water withdrawn from storage tank. The parameters studied are collectors heat gain, heat rejected from coils to shell side of the storage tank, average temperature of storage tank, friction factor, pressure drop, heat exchanger effectiveness, and collector efficiency for circulating mass flow rates of (1.8, 3, 6, 9 l/min), with no water consumption during a clear days in Baghdad. A FORTRAN 95 computer program was developed to evaluate theoretically the pressure drop across the helical coil and to process the experimental data. The results show that heat transfer inside helical coiled tubes is increased with increasing the circulation flow rates and coil diameter ratio. A transition from laminar to turbulent flow has been noticed at (6 and 9 l/min) circulation flow rates. For circulation flow rate of (6 l/min) the transition from laminar to turbulent flow is faster indicated for the outer coil than that for central coil, while the flow is laminar for inner coil. For (9 l/min) circulation flow rate the transition from laminar to turbulent has been noticed for all coils. Collector efficiency is increased with increasing circulation flow rates. The pressure drop decreases with the increase of solar radiation. Friction factor decreases with increasing circulation flow rate. The shell-triple concentric helical coil heat exchanger is found more effective than shell-single coil heat exchanger when the experimental results are compared with previous related work.

Keywords: Solar hot water, Storage tank, Heat exchanger, Helical coil tube, Pressure drop, Effectiveness

1. Introduction

Heat exchangers are used in a wide variety of applications including power plants, nuclear reactors, solar energy, refrigeration and air conditioning systems, automotive industries, heat recovery systems, chemical processing, and food industries. Heat transfer enhancement enables to reduce the size of the heat exchanger. The previously used enhancement techniques can be divided into two groups: active and passive techniques. The active techniques require external actions like fluid vibration, electric field, and surface vibration. The passive techniques require special surface geometries or fluid additives like various tube inserts or utilizing nanofluid. Several studies have indicated that helically coiled tubes are superior to straight tubes when employed in heat transfer applications. The centrifugal force due to the curvature of the tube results in the secondary flow development which enhances the heat transfer rate.

Seban and McLaughlin (1962) presented friction and heat transfer results for the laminar flow of oil and the turbulent flow of water in coiled tube having ratios of coil diameter to tube diameter of 17 and 104, for Reynolds number ranged from 12 to 65000. Rogers and Mayhew (1964) reported experimental results for forced convection heat transfer and friction factors, for water flowing through heated coils. Janssen and Hoogendoorn (1978) studied experimentally and numerically the convective heat transfer in coiled tubes for coil to tube diameter ratios from 10 to 100, Prandtl numbers from 10 to 500 and Reynolds number from 20 to 4000. The heat transfer has been studied for two boundary conditions: for a uniform peripherally averaged heat flux and for a constant wall temperature focusing on the heat transfer in both the thermal entry region as well as the fully developed thermal region. Ali (1994) obtained average outside heat transfer coefficients for turbulent heat transfer from vertical helical coils submerged in water. The coil side heat transfer coefficients are calculated based on the Nusselt number correlation of Rogers and Mayhew (1964). Five different pitch-to-helical diameter ratios were used, along with two tube diameters and with different numbers of turns. He found that increasing the tube diameter for the same Rayleigh number and tube length will enhance the outer heat transfer coefficients. Naphon and Suwagrai (2007) tested coiled tube with three different curvature ratios of 0.02, 0.04, 0.05 under constant wall temperature for heat transfer and flow developments in the horizontal spirally coiled tubes. They employed a finite volume method with an unstructured nonuniform grid system for solving the turbulent flow and heat transfer. The simulated results are compared with the experimental results and a reasonable agreement is obtained. The heat transfer characteristics of shell-helical coiled tube heat exchangers have been investigated

experimentally (Salimpour 2008 and 2009, Shokouhmand 2008, Ghorbani 2010, and Moawed 2011), and computationally [Jayakumar 2011, Ferng 2012], at different design parameters (tube diameter, coil diameter and coil pitch). Kharat, et al. (2009) developed a correlation for heat transfer coefficient for flow of hot flue gases between two concentric helical coils connected in series. They introduced the effect of coil gap in their correlation besides the effect of Reynolds and Prandtl numbers. Hashemi and Bahabadi (2012) carried out an experimental investigation of heat transfer and pressure drop of nanofluid flow inside helical coiled tube under constant heat flux. They found an increase in both heat transfer coefficient and pressure drop by using helical coiled instead of straight tube. Rainieri et al. (2012) investigated experimentally the forced convective heat transfer in straight and coiled tubes having smooth and corrugated wall for two highly viscous fluids (Glycerol and Ethylene Glycol). They concluded that the wall curvature of tube enhances the heat transfer at all Reynolds number, whereas the wall corrugation enhances heat transfer in the higher Re No. range only.

In Solar Hot Water System (SHWS) the solar collector converts the solar radiation to thermal energy which is transferred in a closed loop to the hot water storage tank. Different types of thermal storage tanks have been used for SHWS. Dahl and Davidson (1998) used external tube and shell heat exchanger. Special solar thermal storage tanks are used with horizontal (1998) and vertical (2004) mantle heat exchanger. Furbo et al. (2005) utilized smart solar tank in which the water is heated by solar collectors with auxiliary electrical heater. Mondol et al. (2011) studied the operating characteristics of Solasiphon heat exchanger under indoor and outdoor conditions.

The aim of this work is to investigate the operating thermal and hydrodynamic characteristics of shell- triple concentric helical coiled tube heat exchanger used as a storage tank in forced closed loop solar water heater under outdoor tests for Baghdad climate conditions. Experiments are carried out to analyze the effect of circulating flow rates of (1.8, 3, 6, and 9 l/min) on the collector efficiency and the effectiveness of the storage tank. Up to our knowledge there is no previous reported work dealing with this type of work.

2. Experimental Setup and Procedure

Fig.(1) shows a schematic diagram of the experimental set-up. A closed loop forced circulation solar hot water system is consist of two flat plate solar collectors (in parallel connection), of single glass cover, south oriented, (each of dimensions 1.92m * 0.85m) used to provide hot water stream to a storage tank formed of shell-triple concentric helical coiled tubes. A cold supply water stream (flowing in the shell-side of the storage tank of 120 liter capacity) cools the hot circulating flow rate. The heat exchanger includes a triple copper vertical helical coiled tube shared in single inlet and single outlet. This coil is placed in an insulated cylindrical shell. Specifications of the heat exchanger are depicted in Table 1. A centrifugal water pump type Vicounte PKM60 of (0.5HP) power, is used to circulate water within the closed cycle. Five control valves are used to control the flow rate of hot water and supply coolant water.

The experimental set-up is well instrumented. Fourteen calibrated thermocouples (type K) are located at different positions of the test rig as shown in Fig.(1). All thermocouples are connected to two 12-channels thermometers (type k temperature reader with SD Card Data-Logger-Model BTM-4208SD-Lutron Company) of (0.1 °C) resolution.

A flow meter type Z-4002 float type of range (1.8 to 18 l/min) and (0.3 l/min) resolution is used through this work.. The pressure drop of hot water flows in the helical coiled tubes is measured by using Borden gage of range (0 to 160 mbar) and resolution of (5 mbar). The global solar radiation has been taken from the Ministry of Science and Technology for Baghdad city 33.3° North.

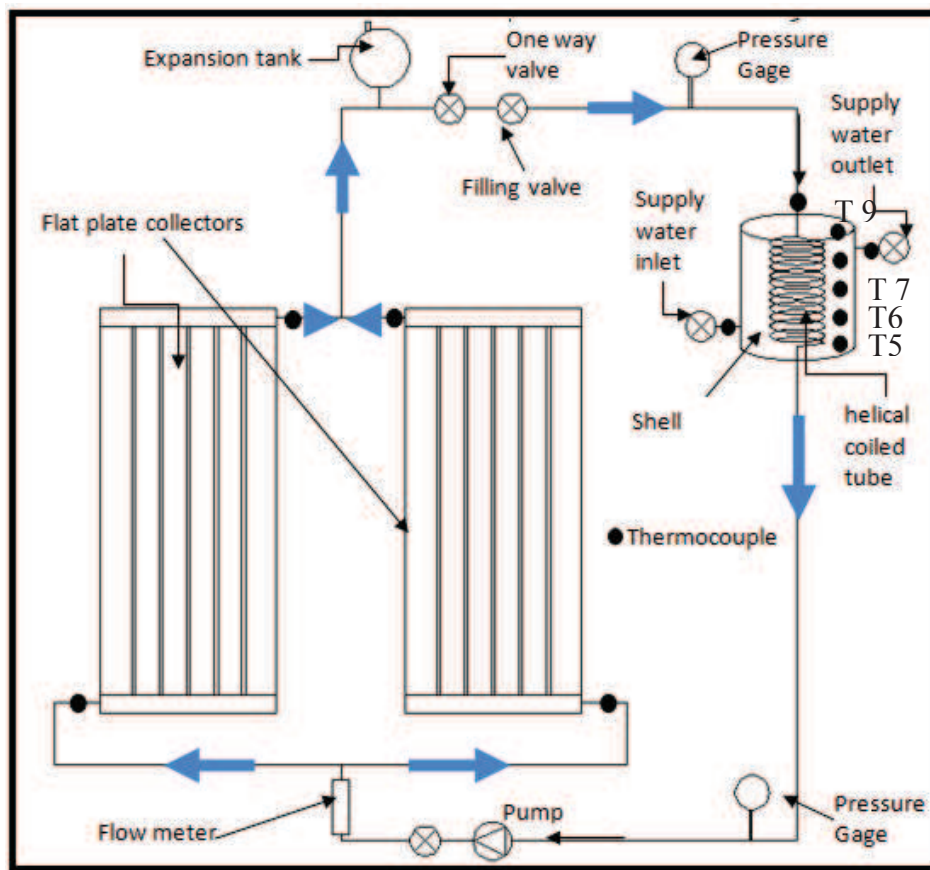


Figure 1. Schematic diagram of the experimental setup
 (Solar Water Heating System SWHS)

Table 1 Geometrical characteristics of the triple concentric coils

Item	Outer Coil	Middle Coil	Inner coil
Coil diameter, tube-center-to-tube-center D_c (mm)	207	152.5	97
tube outside diameter d_o (mm)	12.5	12.5	12.5
tube inside diameter d_i (mm)	10	10	10
Axial length of helical coil L_c (m)	14.95	14.85	14.04
Number of turns in helical coil, N	23	31	46
Curvature ratio, d_i/D_c	0.048	0.066	0.1031
Coil pitch, p (mm)	20	15	10

3. Uncertainty Analysis

The estimated experimental uncertainty in this work is based on the approach presented in Holman (1988). The individual experimental uncertainty of the main measured variables and calculated parameters are given in Table 2. The maximum percentage errors for the parameters involved in the analysis are summarized in Table 3.

Table 2 uncertainty of measured variables

Variable	Temperature	Pressure drop	Flow rate	length	Solar radiation	Water Properties			
						thermal conductivity	density	specific heat	viscosity
Uncertainty %	0.223	4	5.556	0.05	1.3	0.1	0.1	0.1	0.1

Table 3 uncertainty of parameters

Variable	Reynolds No., Re	Nusselt No., Nu	Friction factor, f	Collector efficiency, η	helical coil number He
Uncertainty %	5.56	4.15	11.8	5.713	5.56

4. Theory

4.1 Thermal Analysis

The total amount of heat transferred from coil side is calculated based on the mass flow rate, \dot{m} , the specific heat of water, C_p , and the difference in inlet temperature, T_{ci} , and outlet temperature, T_{co} , given by: Prabhanjan et al. (2004)

$$Q_c = \dot{m} c_p (T_{ci} - T_{co}) \quad (1)$$

The mass flow rate of hot water is calculated as

$$\dot{m} = \rho \dot{V} \quad (2)$$

where

\dot{V} is the volumetric flow rate (m³/s)

ρ is water density at coil side average temperature $(T_{ci} + T_{co})/2$ (kg/m³)

the heat transfer rate Q_c is then used to calculate the overall heat transfer coefficient U ,

$$U = Q_c / [A_o (LMTD)] \quad (3)$$

where

LMTD is the log-mean temperature difference (K), it is evaluated as

$$LMTD = \frac{(T_{ci} - T_{co})}{\ln \left(\frac{T_{ci} - T_{\text{tank,avg}}}{T_{co} - T_{\text{tank,avg}}} \right)} \quad (4)$$

$T_{\text{tank,avg}}$ is tank average temperature (K)

A_o is the outside surface area of the coil (m²), it is calculated as $A_o = \pi d L$

The overall heat transfer coefficient can be rewritten in terms of thermal resistances as,

$$\frac{1}{U A_o} = \frac{1}{h_i A_i} + \frac{\ln(d/d_i)}{2\pi k L} + \frac{1}{h_o A_o} \quad (5)$$

where

h_i is internal heat transfer coefficient inside the coil (W/m².K)

d_i is inside diameter of the coiled tube (m).

d is outside diameter of the coiled tube (m).

A_i is inside area of the coiled tube (m²), $A_i = \pi d_i L$

L is length of the coiled tube (m)

k is thermal conductivity of coiled tube (W/m.K)

Hence the outside heat transfer coefficient (shell side heat transfer coefficient) can be calculated as:

$$\frac{1}{h_o} = \frac{1}{U} - \frac{d}{h_i d_i} + \frac{\ln(d/d_i)}{2\pi k L} \quad (6)$$

In this work the internal heat transfer coefficient, h_i , is evaluated from Nusselt number inside helical coiled tube, Nu_i , which can be predicted according to the value of Reynolds No. inside the coil. The critical Reynolds No. for helical tubes, $Re_{critical}$, related to the curvature ratio is given as: Seban (1962)

$$Re_{critical} = 2 * 10^4 \left(\frac{d}{D_c} \right)^{0.32} \quad (7)$$

The Nusselt number correlation for laminar flow in helical coiled tube is given as: Ghorbani et al. (2010), Bandy et al. (2010)

$$Nu_j = \left[\left(\frac{48}{11} + \frac{51/11}{1 + \frac{1842}{Pr He^2}} \right)^3 + 1.816 \left(\frac{He}{1 + \frac{1.15}{Pr}} \right)^{3/2} \right]^{1/3} \quad (8)$$

and for turbulent flow in helical coiled tube as: Rogers et al. (1994), Ali 1994, Prabhanjan et al. (2004)

$$Nu_j = 0.023 Re^{0.85} Pr^{0.4} \left(\frac{d}{D_c} \right)^{0.1} \quad (9)$$

where

Pr is Prandtl number

Re is Reynolds number = $\frac{\rho V d_i}{\mu}$

μ is water dynamic viscosity at coil side average temperature (N.s/m²).

V is water velocity inside coiled tube (m/s).

He is helical coil number defined as $He = Re \sqrt{\frac{d}{D_c}} \left[1 + \left(\frac{p}{\pi D_c} \right)^2 \right]^{-1/2}$.

d is coiled tube outside diameter (m).

D_c is coil diameter (m).

p is coil pitch (m).

The inside heat transfer coefficient can be calculated as:

$$h_j = \frac{Nu_j k}{d_i} \quad (10)$$

The effectiveness of the storage tank can be expressed as: Klett et al. (1984)

$$\varepsilon = \frac{(T_{ci} - T_{co})}{(T_{coil,i} - T_{tank,avg})} \quad (11)$$

The collector efficiency, η , can be calculated as: Duffi and Beckman (1974)

$$\eta = \frac{\dot{m} \dot{C}_p \Delta T}{AI} \quad (12)$$

where

ΔT is collector outlet and inlet temperature difference (K)

A is the area of collectors (m²)

I is incident solar radiation (W/m²)

3.2 Hydrodynamic Analysis

The friction factor for laminar flow inside helical coiled tube can for a range of Dean number (De) of (11.6 < De < 2000) is correlated as: Seban and Mclauchlin (1962)

$$\frac{f}{f_s} = \left[1 - \left[1 - \left(\frac{11.6}{De} \right)^{0.45} \right]^{2.22} \right]^{-1} \quad (13)$$

where

$$De = Re \sqrt{d/D_c} \quad (14)$$

f_s is friction factor for straight tube, it is calculated for laminar flow as $f_s = \frac{64}{Re}$

The friction factor for turbulent flow in helical coiled tube, f, is determined as: Seban and Mclauchlin (1962)

$$\frac{f}{f_s} = \left[Re \left(\frac{d}{D_c} \right)^2 \right]^{1/20} \quad \text{for } Re \left(\frac{d}{D_c} \right)^2 > 6 \quad (15)$$

where

$$f_s/8 = 0.023 (Re)^{-0.2}$$

The pressure drop of water flowing inside the coiled tubes is evaluated as

$$\Delta p = f_p \frac{L}{d_i} \frac{v^2}{2} \quad (16)$$

5. Results and discussion

Fig.2 illustrates the total solar radiation on the collector plane, the ambient temperature and wind speed on 19th of March 2012 (clear day) measured in Baghdad Lat. 33.3° North, Long. 33° East. The ambient temperature rises with the increase of the solar radiation. The maximum ambient temperature was (20.8°C) at 3:00 PM, while inconsiderable variation in wind speeds is indicated. The global solar radiation was (178W/m² and 612W/m²) at 8:00AM, and 12:00 AM respectively.

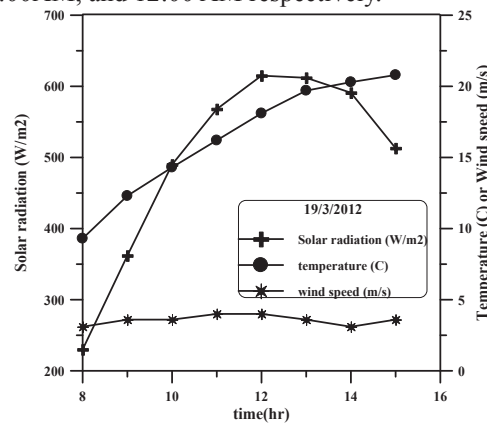


Figure 2. Hourly variation of solar radiation , ambient temperature, and wind speed.

Fig. 3a,b,c,d shows the inlet and outlet temperature of hot water through the flat plate solar collector for different circulation flow rates. The temperature difference across the collector decreases as circulating flow rate increases. The temperature difference at 12:00PM was (10.1°C, and 2.8°C) for mass flow rate (1.8, and 9 l/min) respectively. The thermal stratification profile in the storage tank is illustrated in Fig.(4). A uniform increase in average water temperature following the solar radiation is shown with slight variation with circulating flow rate.

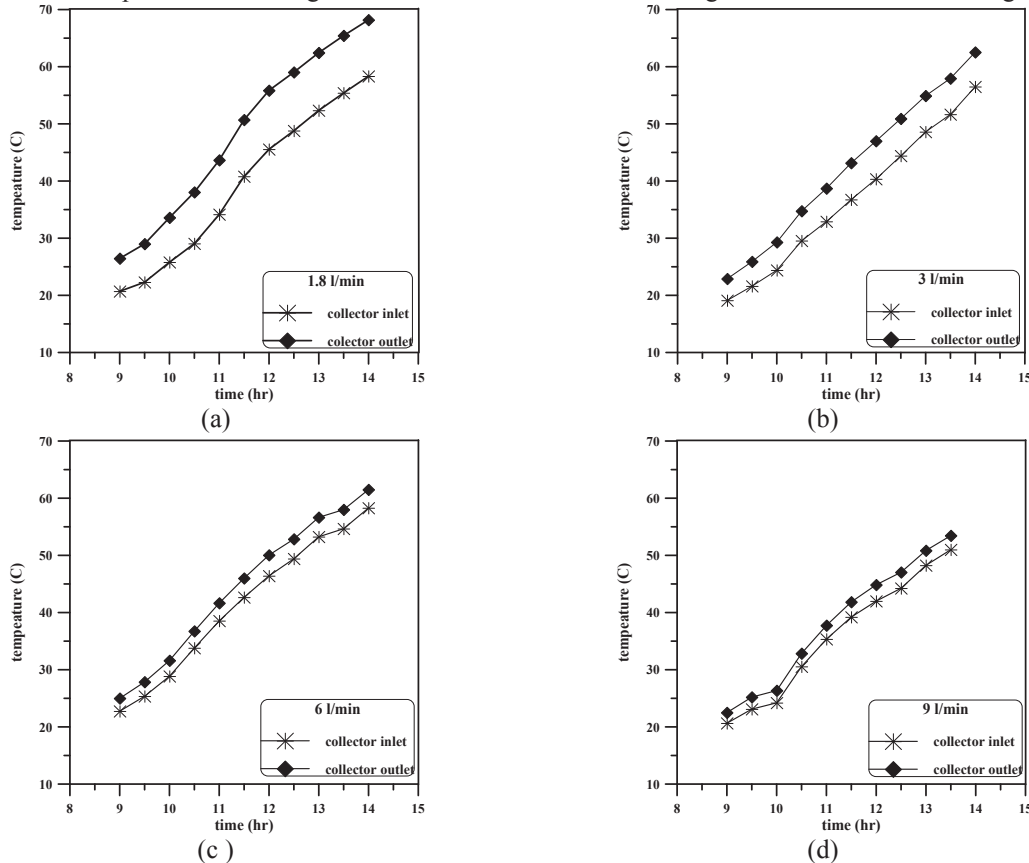


Figure 3. Variation of hourly inlet and outlet water temperature for solar collector.
 a)1.8 l/min, b)3 l/min, c)6 l/min, d)9 l/min

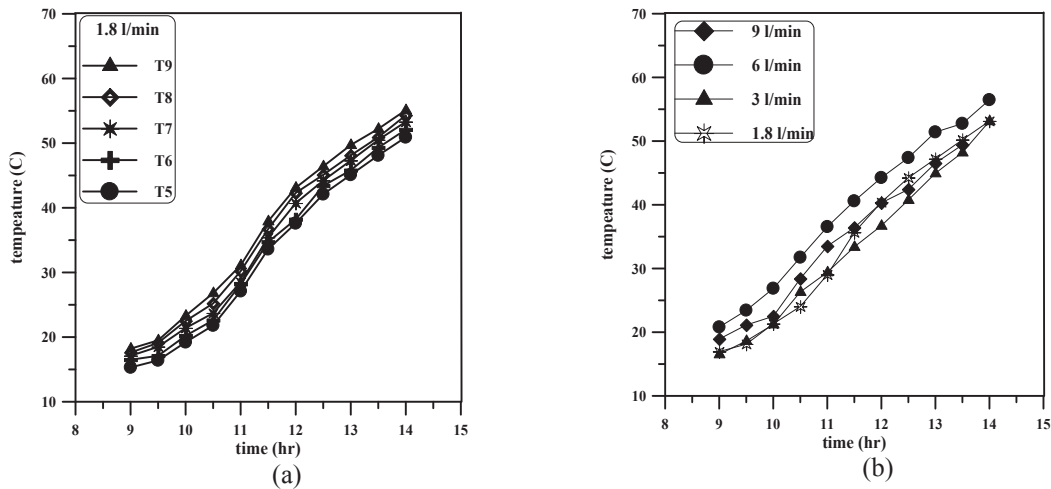


Figure 4. Water temperature within shell side a) Thermal stratification at 1.8 l/min, b) Average temperature at various circulation flow rates

Fig. 5a,b illustrates the time variation of collector heat gain (Q_{gain}) and the heat transferred from the coil side to the shell side of the storage tank (Q_{coil}) at various circulating flow rates. An increase in (Q_{gain}) and (Q_{coil}) with the increase of the circulation flow rate is noticed. The collector heat gain is higher than coil heat rejected to the shell side since part of the heat is lost to the ambient. The values of (Q_{gain}) are (1276, 1376, 1509, and 1770 W) and (Q_{coil}) are (1251, 1325, 1447, and 1739 W) at 12:00AM for circulating flow rates of (1.8, 3, 6, and 9) respectively.

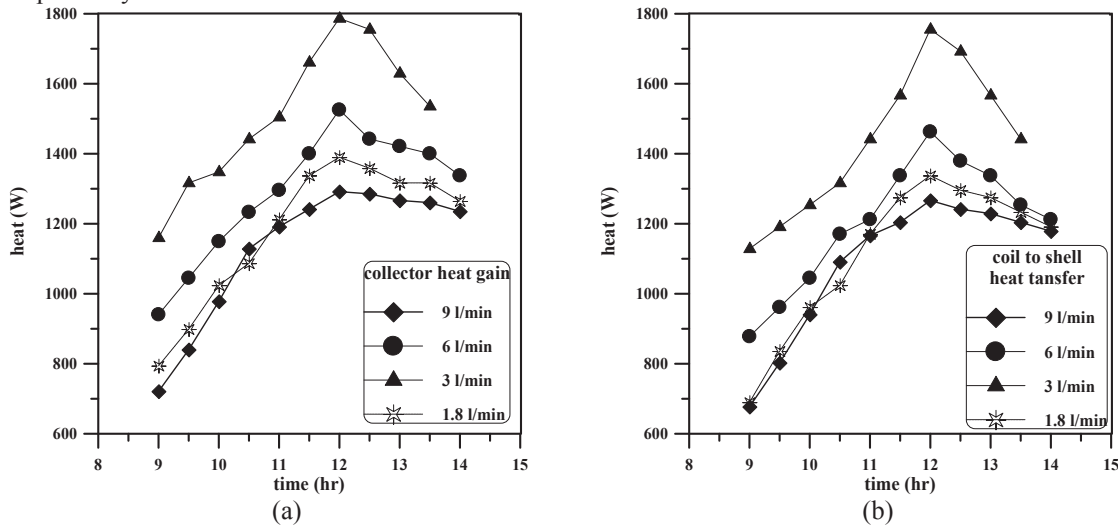


Figure 5. Variation of hourly, a)Collector heat gain, b) Heat transferred from coil to shell side.

The collector efficiency increases with the increase of circulation flow rates as shown in Fig. 6. Since the increase of the circulation flow rate leads to increase Reynolds No. which increases Nusselt No. and heat transfer coefficient so higher heat gain can be obtained. The collector efficiency reaches (52.7%, 55.3%, 69%, and 71.6%) at 12:00 PM for flow rates of (1.8, 3, 6, and 9 l/min) respectively. The storage tank effectiveness follows the incident solar radiation, and it rises with decreasing the circulation flow rate as presented in Fig. 7.

The inside Nusselt No. increases with increasing Dean No. for inner, middle and outer coils at different circulating flow rates as reported in Fig. 8a,b,c,d. Higher values of inside Nusselt No. are for inner coil (of coil diameter to tube diameter ratio of 9.7) for (1.8 and 3 l/min) circulating flow rates as reported in Table 4. A steep increase in Nusselt No. at the transition from laminar to turbulent flow for circulating flow rates of (6 and 9 l/min) with higher values indicated for outer coil as illustrated in Fig. 8c and 8d.

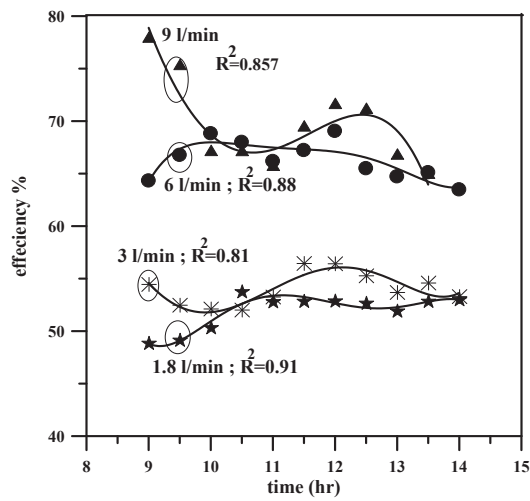


Figure 6. Hourly variation of collector efficiency for different circulation flow rates

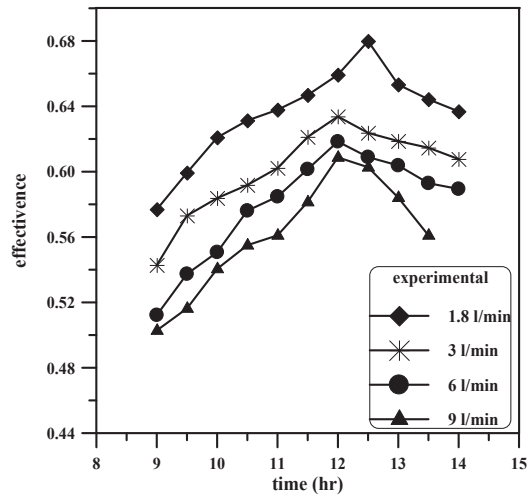


Figure 7. Hourly variation of storage tank effectiveness for different circulation flow rates

Table 4 Hourly experimental helical coil side Nusselt Number

Circulation Flow rate	1.8 l/min			3 l/min			6 l/min			9 l/min		
	inner coil	middle coil	outer coil	inner coil	Middle coil	outer coil	inner coil	middle coil	outer coil	inner coil	middle coil	outer coil
9:00	25.8	23.1	21.5	32.3	28.9	26.8	46.8	41.9	38.8	56.1	50.1	46.5
9:30	26.3	23.6	21.9	33.1	29.7	27.5	48	42.9	39.8	57.3	51.2	47.5
10:00	27.2	24.4	22.7	34.1	30.5	28.3	49.6	44.3	41.1	58.1	51.9	48.1
10:30	28	25.1	23.3	35.7	31.9	29.6	51.6	46.1	42.7	61.4	74.9	72.7
11:00	29.2	26.2	24.3	36.7	32.9	30.5	53.5	47.8	44.3	63.7	77.8	75.4
11:30	30.6	27.4	25.4	37.9	33.9	31.4	55	49.1	45.5	83.2	79.5	77.1
12:00	31.5	28.2	26.1	38.8	34.7	32.2	56.3	50.3	58.1	85.7	81.9	79.4
12:30	32	28.7	26.6	39.8	35.6	33	57.3	51.2	59.2	86.9	83.1	80.6
13:00	32.6	29.2	27.1	40.8	36.4	33.8	58.6	62.6	60.7	89.2	85.3	82.7
13:30	33.1	29.6	27.5	41.5	37.1	34.4	59	63	61.1	90.8	86.8	84.2
14:00	33.6	30	27.9	42.5	38	35.2	60.1	64.4	62.5			

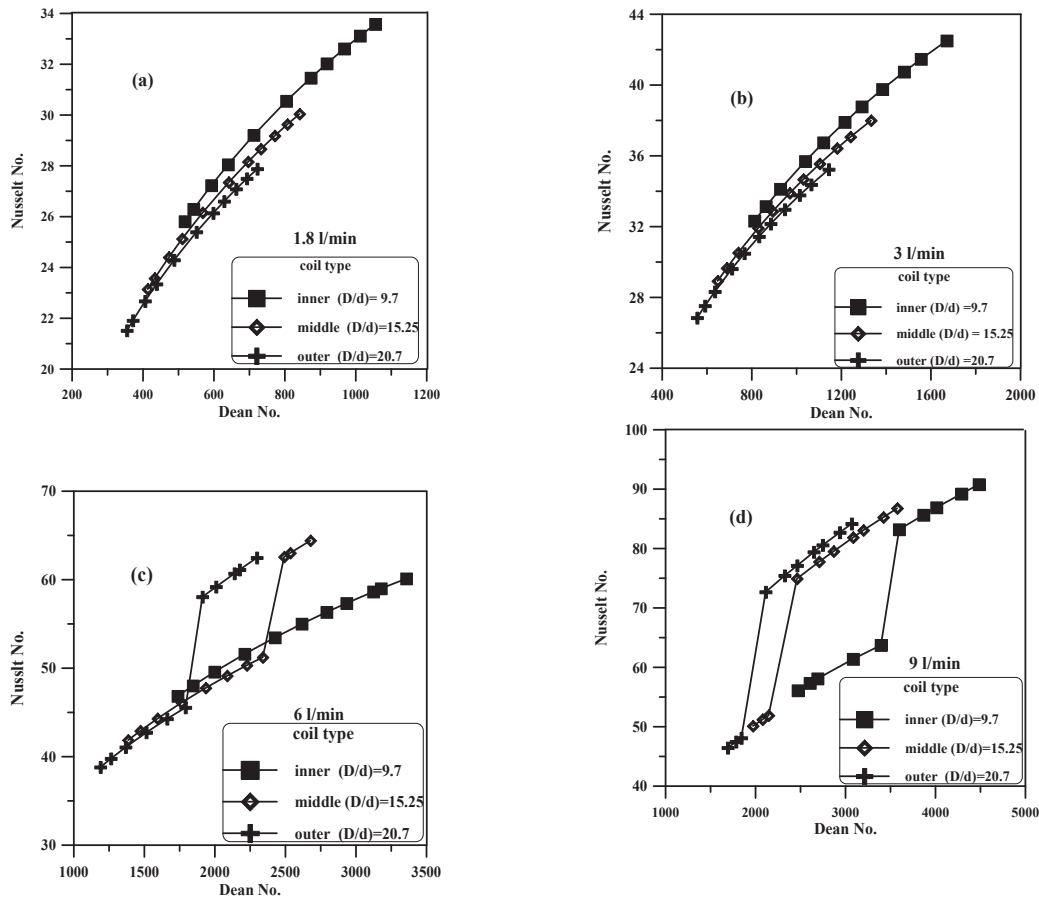


Figure 8. Variation of hourly Nusselt no. for different circulation flow rates
 a) 1.8 l/min, b) 3 l/min, c) 6 l/min, d) 9 l/min

The transition from laminar to turbulent flow is starts first in outer coil then middle coil and finally in inner coil. Fig. 9 clears that the average inside Nusselt No. of the triple helical coil increases with increasing circulating flow rates and Dean No.

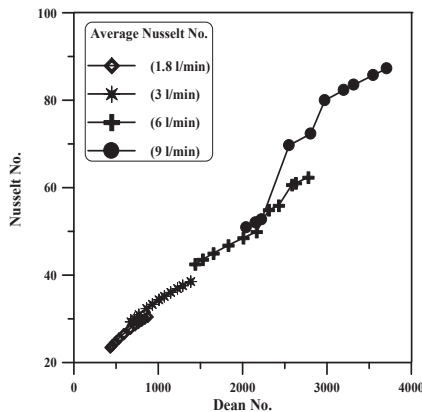


Figure 9. Variation of average inside Nusselt No. at different circulating flow rates.

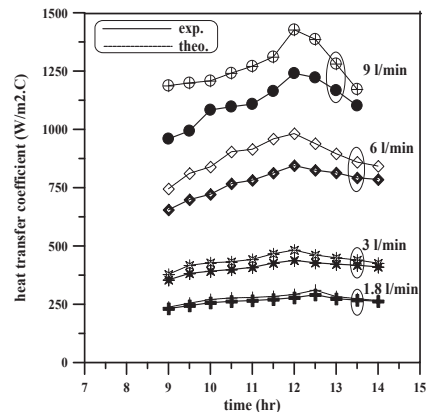


Figure 10. Variation of hourly shell side heat transfer coefficient.

Fig. 10 shows an increase of shell side heat transfer coefficient (h_o) with the increase of circulation mass flow rate and it follows the solar radiation. The deviation between the theoretical and experimental shell side heat transfer coefficient increases as circulating flow rate is increased. The range of this deviation was (1.14% to 6.32%) and (6% to 19.2%) for circulation flow rates of (1.8 l/min) and (9 l/min) respectively.

The measured pressure drop across the triple concentric helical coiled tube increases with the increase of circulating flow rate, as shown in Fig. 11. It can be seen that the pressure drop decreases for 5 hours of heating

period. This is because of the decrease of water density and viscosity with increasing water temperature.

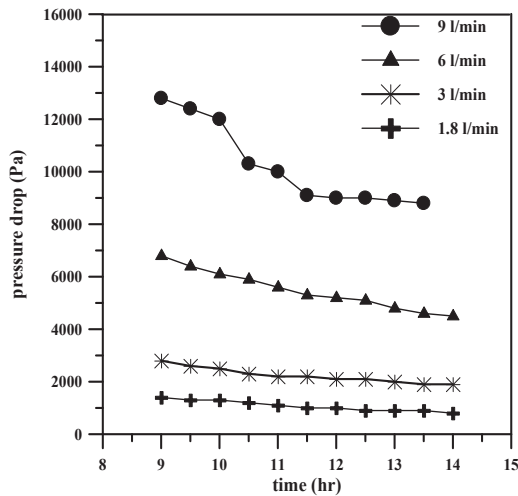


Figure 11. Variation of measured pressure drop across helical coiled tube

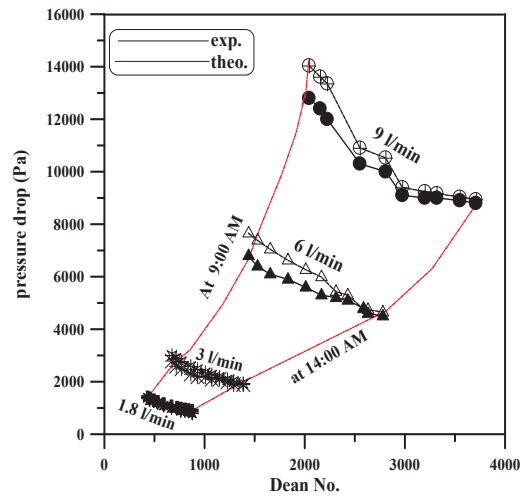


Figure 12. Hourly variation of pressure drop inside helical coiled tube.

Fig.12 shows good agreement between experimental and theoretical values of pressure drop across the triple concentric coil at (1.8 and 3 l/min) circulating flow rates. Some deviation at the first 3 hours can be noticed for (6, and 9 l/min) flow rates. It is found that the pressure drop decreases with the increase of Dean Number for each flow rate of circulations.

A good agreement between the theoretical and experimental friction factor is obtained as shown in Fig. 13, with a percentage deviation of (1.2, 3.6, 0.78, and 1.4) at flow rates of (1.8, 3, 6, and 9 l/min) respectively at 12:00 AM.

Again good agreement between the theoretical and experimental friction factor for all values of circulating flow rates is shown in Fig(14). The minimum and maximum deviations were (0.17% and 9.5%) respectively.

Since there is a rare work matches the parameters studied in this study, the heat gain to heat input ratio at (3 l/min) circulating flow rate of the present work is compared with the results of Mondol (2012) for single coil-shell storage tank (119.6 liter) at (2.4 l/min) circulating flow rate as shown in Fig. 15., the triple concentric coiled tube is more efficient than the single coil tube.

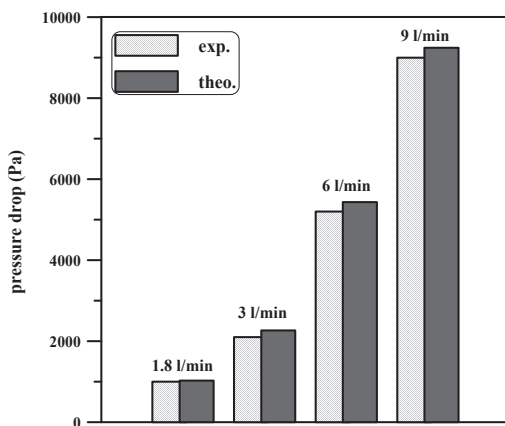


Figure 13. Theoretical and experimental pressure drop across concentric helical coiled tubes at 12:00 PM.

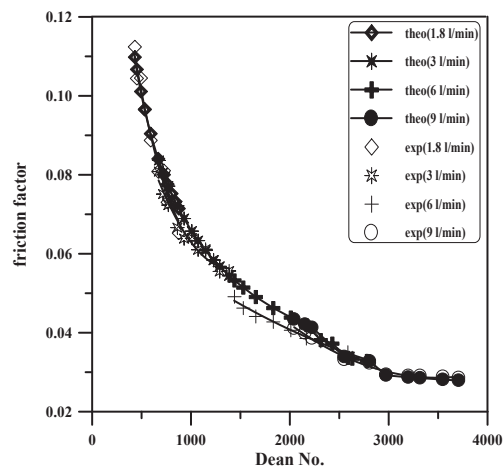


Figure 14. Variation of theoretical and experimental friction factor inside concentric helical coiled tube.

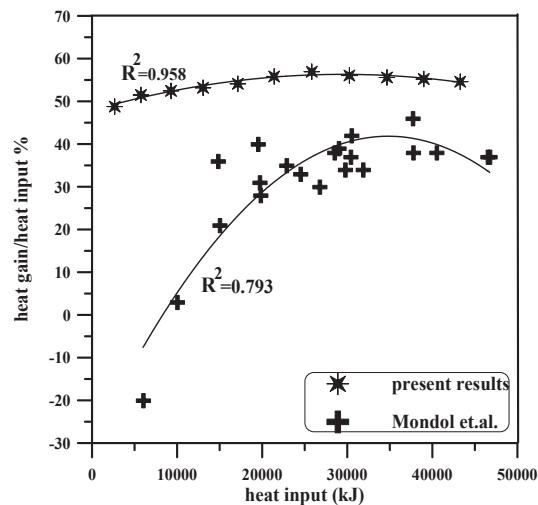


Figure 15. Comparison of the percentage heat transfer of the present work with results reported by Mondol et al. (2011).

6. Conclusions

The performance of novel heat exchanger unit developed for a solar water heater has been investigated under outdoor conditions. Following the experimental investigation, a number of conclusions can be extracted:

1. A weak variation of temperature difference across the collector inlet and outlet during the test day for higher values of circulating flow rates.
2. The circulation rate is a significant parametric effect on the useful heat gain of the collector. The maximum heat gain was (1750W) at (12:00PM) for (9 l/min).
3. The efficiency of the collector increases with the increase of circulation mass flow rate. High values of collector efficiency are obtained since the distribution of the triple helical coils within the shell assists to reject heat to the shell side and allows the fluid to return cooler to the collectors and increases the collector efficiency. The collector efficiency range was (48% to 78%).
4. Effectiveness of heat exchanger is increased when circulation flow rate is decreased. The heat exchanger effectiveness follows the solar radiation.
5. Inside Nusselt number increases with increasing Dean Number therefore increasing of tube diameter to coil diameter ratio leads to increase Nusselt number.
6. The transition from laminar to turbulent flow is found for high circulation flow rates namely (6 l/min and 9 l/min). For circulation flow rate of (6 l/min) the transition from laminar to turbulent flow is indicated for outer coil faster than central coil, while the flow was laminar in inner coil. For circulation flow rate of (9 l/min) the transition from laminar to turbulent is shown for all coils, but the turbulent flow starts in the outer then the central and finally in the inner.
7. The hourly pressure drop decreases when Dean No. increases for each circulation flow rate.
8. The water density and viscosity decreases with increasing solar radiation which leads to increase the Dean No. with day hours.
9. The friction factor inside helical coiled tube increased when flow rate of circulation decreased.

Reference

- Ali, M.E. (1994), "Experimental investigation of natural convection from vertical helical coiled tubes", *Int. J Heat Mass Transfer* 37(4), 665-671.
- Bandpy, M.G. & Sajjadi, H. (2010), "An experimental study of the effect of coil step on heat transfer coefficient in shell-side of shell-and-coil heat exchanger", *World Academy of Science, Eng. and Tech.* 71, 364–369.
- Dahl, S.D. & Davidson, J.H. (1998), "Mixed convection heat transfer and pressure drop correlations for tube in shell thermosyphon heat exchangers with uniform heat flux", *ASME J. of Solar energy engineering* 120, 260-269.
- Duffi, J.A. & Beckman, W.A. (1974), "Solar Energy Thermal Process", John Wiley & sons Inc. New York.
- Ferng, Y.M., Lin, W.C., Chieng, C.C. (2012), "Numerically investigated effects of different Dean number and pitch size on flow and heat transfer characteristics in a helically coil-tube heat exchanger", *Applied Thermal Engineering* 36, 378-385.
- Furbo, S., Andersen, E., Knudsen, S., Vejen, N.K., Shah, L.J. (2005), "Smart solar tanks for small solar domestic

- hot water systems", *Solar Energy* 78, 269–279.
- Ghorbani, N., Taherian, H., Gorji, M., Mirgolbabaie, H. (2010), "An experimental study of thermal performance of shell-and-coil heat exchangers", *Int. Comm in Heat and Mass Transfer* 37, 775–781.
- Hashemi, S.M., Akhavan-Behabadi, M.A. (2012), "An empirical study on heat transfer and pressure drop characteristics of CuO–base oil nanofluid flow in a horizontal helically coiled tube under constant heat flux", *Int. Comm in Heat and Mass Transfer* 39, 144–151.
- Holman, J.P. (1988), "Experimental methods for engineers", 5th edition, McGraw-Hill.
- Janssen, L.A.M., Hoogendoorn, C.J. (1978), "Laminar convective heat transfer in helical coiled tubes", *Heat Mass transfer* 21, 1197-1206.
- Jayakumar, J.S., Mahajani, S.M., Mandal, J.C., Iyer, K.N., Vijayan, P.K. (2010), "CFD analysis of single-phase flows inside helically coiled tubes". *Computers and Chemical Eng.* 34, 430–446.
- Kharat, R., Bhardwaj, N., Jha, R.S., (2009), "Development of heat transfer coefficient correlation for concentric helical coil heat exchanger", *Int. J of Thermal Sciences* 48, 2300–2308.
- Klett, D.E., Goswami, D.Y., Saad, M.T. (1984), "Thermal performance of submerged coil heat exchangers used in solar energy storage tanks", *J. of Solar Energy Engineering* 106, 373-375
- Knudsen, S. & Furbo, S. (2004), "Thermal stratification in vertical mantle heat exchangers with application to solar domestic hot-water systems", *Applied Energy* 78, 257-272.
- Kumar, V., Saini, S., Sharma, M., Nigam, K.D.P. (2006), "Pressure drop and heat transfer study in tube-in-tube helical heat exchanger", *Chem. Eng. Science* 61, 4403–4416.
- Moawed, M., (2011), "Experimental study of forced convection from helical coiled tubes with different parameters", *Energy Conversion and Management* 52, 1150–1156
- Mondol, J.D., Smyth, M., Zacharopoulos, A. (2011), "Experimental characterization of a novel heat exchanger for a solar hot water application under indoor and outdoor conditions", *Renewable Energy* 36, 1766-1779.
- Morrison, G.L., Nasr, A., Behnia, M., Rosengarten, G. (1998), "Analysis of horizontal mantle heat exchangers in solar water heating systems", *Solar Energy* 64(1–3), 19–31.
- Naphon, P., Suwagrai, J., (2007), "Effect of curvature ratios on the heat transfer and flow developments in the horizontal spirally coiled tubes", *Int. J Heat and Mass Transfer* 50, 444–451.
- Prabhanjan, D.G., Rennie, T.J., Raghavan, G.S.V. (2004), "Natural convection heat transfer from helical coiled tubes", *Int J of Thermal Sciences* 43, 359-365.
- Rainieri, S., Bozzoli, F., Pagliarini, G. (2012), "Experimental investigation on the convective heat transfer in straight and coiled corrugated tubes for highly viscous fluids: Preliminary results", *Int J of Heat and Mass Transfer* 55, 498–504.
- Rogers, G.F.C, Mayhew, Y.R., (1964), "Heat transfer and pressure loss in helically coiled tubes with turbulent flow", *Int. J Heat Mass Transfer* 7, 1207-1216.
- Salimpour, M.R. (2008) "Heat transfer characteristics of a temperature-dependent-property fluid in shell and coiled tube heat exchangers", *Int. Comm. in Heat and Mass Transfer* 35,1190–1195.
- Salimpour, M.R., (2009), " Heat transfer coefficients of shell and coiled tube heat exchangers", *Experimental Thermal and Fluid Science* 33, 203–207.
- Seban, R.A., Mclauchlin E.F. (1962), "Heat transfer in tube coils with laminar and turbulent flow", *Heat mass transfer* 6, 387-395.
- Shokouhmand, H., Salimpour, M.R., Behabadi, M.A. (2008), "Experimental investigation of shell and coiled tube heat exchangers using Wilson plots", *Int. Comm. in Heat and Mass Transfer* 35, 84–92.

Nomenclature

symbol	Description	symbol	Description
A	surface area (m ²)	L	coil length (m)
C _p	specific heat (kJ/kg K)	\dot{m}	mass flow rate (kg/s)
D	helical coil diameter (m)	N	number of coil turns
De	Dean number	Nu	Nusselt No.
d	outside tube diameter (m)	P	coil pitch (m)
f	friction factor	Δp	pressure drop (Pa)
g	gravitational acceleration (m/s ²)	Q	heat transfer (W)
h	heat transfer coefficient (W/m ² K)	T	temperature (°C)
I	solar radiation (W/m ²)	UA	overall heat transfer coefficient (W)
k	thermal conductivity (W/mK)	V	fluid velocity inside coil (m/s)
Greek symbols			
ϵ	effectiveness	ρ	mass density (kg/m ³)
μ	dynamic viscosity (kg/m.s)	ΔT	temperature difference (°C)
ν	kinematic viscosity (m ² /s)		
subscript			
c	coil	i	inlet
coll	collector	o	outlet
tank,avg.	tank average		